Reconfigurable Photonic Switch Based on a Binary System Using the White Cell and Micromirror Arrays

Victor Argueta-Diaz and Betty Lise Anderson, *Senior Member, IEEE*

***Abstract*—We describe an $N \times N$ optical switch for use in cross-connects. It is a free-space device, based on multiple bounces in a pair of White cells sharing a spatial light modulator at one end. In a companion paper, we described various polynomial cells, in which the number of outputs was proportional to the number of bounces raised to some power. In the binary device described here, the number of possible outputs is proportional to the number two raised to the power of the number of bounces. It allows a 1024 $\times$ 1024 switch using a single digital two-state tip/tilt micromirror array, four spherical mirrors, and a spot displacement device. It is highly scalable and insensitive to micromirror pointing accuracy.**

***Index Terms*—Microelectromechanical systems (MEMS), optical communication, optical interconnects, White cell.**

I. Introduction

THANKS to new sources, new amplifiers, and improved fabrication methods for optical fibers, the transmission capacity of telecommunication transmission systems is exploding. Due to the complexity of optical networks, switching has become an important function for any communication system. Until recently, electronic switches were used to route the information. However, with the huge capacity of today's telecommunication systems, the use of electronic switches becomes cumbersome. When optical signals are switched by electronic devices, they are first converted into an electrical signal, switched electronically, and then converted back into light. These optical-electrical-optical (OEO) conversions introduce unnecessary time delays and bandwidth bottlenecks. The need for a new type of large capacity, wavelength-independent crossconnect switch naturally opened the way to all-optical switches. All-optical switches are those in which there is no OEO conversion required to switch the signal to a different output.

Many approaches to the all-optical crossconnect problem can be found in the literature. In general, they can be divided into planar and three-dimensional (3-D) approaches. In planar approaches, the inputs/outputs are in the same plane as the switching device. Planar approaches include switches based on waveguides, and can be made using electrooptic [1], [2] or thermooptic materials [3]. Planar switches have the advantage that they are easy to manufacture, because planar technology has been used in electronics for quite some time. Another advantage is that because planar designs usually work using waveguides, the coupling between successive stages is less problematic than in free-space approaches. Planar approaches can also be made using free-space and microelectromechanical systems (MEMS) mirror arrays. For example, in [4], a device uses a linear array of input fibers along one edge of the chip and another array along an adjacent edge. Micromirrors pop up and down to divert each beam to its intended destination. A problem with planar switches is that their scalability is limited, mainly because the number of inputs/outputs that can be involved depends on the dimensions of the substrate, and these cannot be made arbitrarily large.

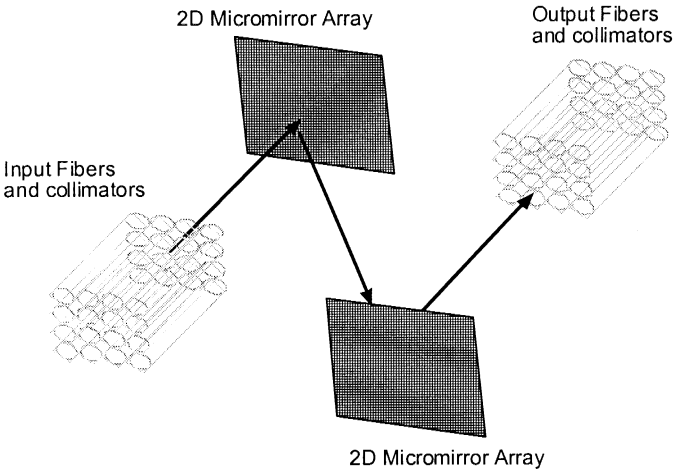

Fig. 1. 3-D optical switch using MEMS mirrors (after [5]).

In 3-D approaches, the inputs and outputs are arranged in a different plane than the switching device, rather than along its sides. Usually, the input/output fibers are in an array facing the switching plane (see Fig. 1) [5]. The input beams are directed perpendicular to a MEMS device composed of an array of micromirrors. Each micromirror can be tilted to different positions; thus, it is possible to control the direction in which each light beam is reflected. Then, the beam is sent to a second MEMS device that directs the beam to a fiber in the output fiber array. Lucent has described a variation of this approach [6] and recently reported a 1024 $\times$ 1024 crossconnect using MEMS devices.

The 3-D approach is ultimately the most scalable and, thus, the most practical long-term solution. Because the 3-D solutions involve free space, however, the beams diverge as they propagate from one element to another. Although the beams can be collimated to some extent, these approaches will be limited in how far a beam can be transmitted before becoming too large. Although switches with small numbers of interconnections (16 $\times$ 16, 32 $\times$ 32) are commercially available, switches with a large number of interconnections are harder to build due to high-precision alignment requirements on the MEMS and large aberrations.

Manuscript received September 24, 2002; revised March 3, 2003.

The authors are with the Department of Electrical Engineering, The Ohio State University, Columbus, OH 43210 USA (e-mail: argueta-diaz.1@osu.edu; Anderson@ee.eng.ohio-state.edu).

Digital Object Identifier 10.1109/JSTQE.2003.813305

The aim of this paper is to propose a highly scalable all-optical 3-D crossconnect switch for a large number of family "exponential cells" in which $N \propto 2^m$ (for the binary case). The binary approach has the advantage of providing far more connectivity for a given number of bounces (and thus, loss), but the disadvantage of not having the built-in redundancy of the polynomial devices.

Our binary device is based on an optical White cell, which has been described in detail elsewhere [7], [8]. In a companion paper [9], we showed how to adapt the White cell to produce an optical switch. There, we discussed several "polynomial" configurations in which the number of outputs that could be reached was proportional to the number of times a given beam bounced in the White cell m, raised to some power. In this paper, we show how to create a switch in which the number of possible outputs is proportional to $2^{m/4}$, which for large m, will always produce more connections.

In the polynomial cells, some number of White cells were combined with a spatial light modulator [we considered an MEMS tipping-mirror switch]. The MEMS switched beams among various White cells, and each objective mirror had a slightly different alignment. This produces shifts of various sizes in the spots produced by the bouncing beams. In the binary cell described here, however, there are only two pairs of objective mirrors. One pair images the spots onto a plain mirror, which does not affect the fundamental spot pattern of the White cell. The other pair of objective mirrors will produce shifts in the spots, which will ultimately cause the beam to emerge from the White cell at a new location.

Specifically, an optical device that we call a spot displacement device (SDD) embedded in the White cell will shift the beam to a new output every time the beam goes to it, creating the binary pattern. We will again use a MEMS device and a system of spherical mirrors that will refocus the beam continuously. A beam will bounce inside this system a specific number of times, and the number of possible outputs will be determined by these bounces.

The organization of this paper is as follows. First, in Section II, we will present an optical switching device with a binary configuration using SDDs and discuss its operation. In Section III, we present a design procedure for finding solutions for SDDs. In Section IV, we will describe some possible physical implementations for the SDD. Finally, in Section V we will give a summary and conclusion.

II. Binary Cell

Our goal is to perform optical switching, which we will do by allowing each of a large number of input beams to be switched between two different White cells. One White cell produces the two rows of spots for each input beam, and the second White cell incorporates an SDD that will continue the spot patterns but displace them by some number of rows, thus changing the exit location of each beam. We must allow for a very large number of potential outputs for each of the input beams, but with a smallest possible number of bounces. Reducing the number of bounces reduces the loss, which will accumulate on every bounce. To this end, we propose a "binary cell," in which the number of outputs is proportional to $2^{m/4}$, where m is the number of bounces in the White cell. Here, we will show how to combine two White cells to produce the interconnection device.

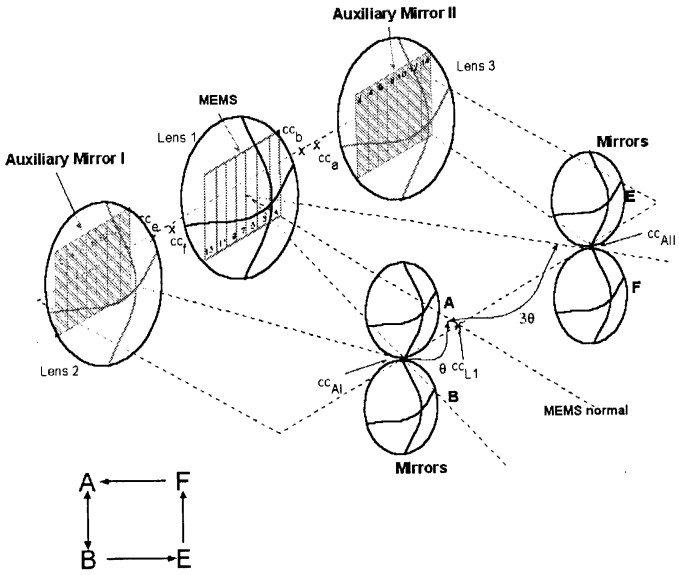

Fig. 2. Binary switch configuration.

In the original White cell, the location at which a spot leaves the cell is determined by where the beam went in, and where the centers of the curvature of Mirrors B and C were. In this section, we will modify the White cell so that we can control the output location. To do this, we will replace Mirror M with a MEMS tilting micromirror array to select between two different paths on each bounce. We will then use an architecture originally proposed by Collins *et al.* [10] for optical true time delay devices for phased array antennas. Thus, we will add an additional White cell in the newly available path. Both White cells produce a similar spot pattern, but in the second White cell, spots are shifted such that they return in a different row than if they are sent to the first White cell.

Fig. 2 shows the new design for the White cell device. Mirror M has been replaced with a MEMS micromirror array and a lens. The lens/MEMS mirror combination performs the imaging function of the original spherical Mirror M. On either side of the MEMS mirror two flat mirrors (Auxiliary Mirrors I and II) are placed; their functions will be described shortly. Each of the auxiliary mirrors also has a field lens to simulate a spherical mirror. These could be combined into a single, larger lens as well. In addition, there are four spherical mirrors on the right instead of two. Instead of having the centers of curvature of the spherical mirrors on the MEMS mirror, the centers of curvature are placed outside the MEMS mirror.

We take the possible micromirror tip angles to be $\pm\theta$. Mirrors A and B are placed one above the other, along an axis at $-\theta$. Mirrors E and F are also placed one above the other along an axis at $+3\theta$. There are two effective centers of curvature of the lens associated with the MEMS mirror, depending on the micromirror tip angle. One is placed between Mirrors A and B, and the other is placed between Mirrors C and D. The center of curvature of Auxiliary Mirror I and its lens is placed between Mirrors A and B, and similarly, the center of curvature of Auxiliary Mirror II and its lens is placed between Mirrors E and F.

Let us assume an input beam going from the MEMS mirror plane is sent to Mirror A, for example after bounce 1. Light coming from this spot is imaged to a new spot on Auxiliary Mirror I (labeled "2"). From there, the light is reflected to Mirror B, which sends the light back to the MEMS at a new location, bounce number 3. If the micromirror at that spot is set to $-\theta$, then the light is sent back to Mirror A again. So, Mirrors A and B form a White cell with the lens 1/MEMS combination, Auxiliary Mirror I, and lens 2.

If a pixel at bounce 3 is then turned to $+\theta$, then light coming from Mirror B to this micromirror will be reflected from the MEMS mirror at an angle of $+3\theta$ with respect to the normal to the MEMS mirror plane. Recall there are two more mirrors along that axis, E and F. So, light coming from B will go to E. Light must always go from an upper mirror to a lower mirror. When light goes to Mirror E, the light is sent to Auxiliary Mirror II, where it forms a spot ("4"). From there, the light is sent to the lower Mirror F, and then back to the MEMS mirror plane. Therefore, Mirror E and F form another White Cell. If the next micromirror in the MEMS device is tilted to $-\theta$, the beam from F is sent again to the AB White cell (specifically to Mirror A). If the micromirror at this point had been tilted to $+\theta$, the light coming from F would have been reflected at $+4\theta$, a direction that is not being used in this design, and the beam is lost.

Thus, according to the connectivity diagram shown in the lower left-hand corner in Fig. 2, light can bounce continuously (and exclusively) between the MEMS and Auxiliary Mirror I via Mirror A and B, a situation that does not occur while bouncing through E and F. Light going to Auxiliary Mirror II gets there via Mirror E and returns to the MEMS via Mirror F. From here light must go to back to Mirror A and Auxiliary Mirror I. Therefore, light returning from Auxiliary Mirror II needs four bounces to go back to Auxiliary Mirror II.

An input beam can be sent to Mirror A from the MEMS mirror plane every even-numbered bounce, and to Mirror E every fourth bounce (i.e., 4, 8, 12 …). The odd-numbered bounces always appear on the MEMS, and the even-number spots can appear either on Auxiliary Mirror I or II. The light can be sent to Auxiliary Mirror II on any particular even-numbered bounce, but if the light is sent there, four bounces are required before it can be sent there again.

Now, we will replace Auxiliary Mirror II with a device that will shift a spot down by some number of rows. The spots will be shifted by this SDD. We will divide Auxiliary Mirror II into columns, one column to every four bounces, and the number of pixels by which a beam is shifted will be different for each column. That is, each column will shift a beam by a distance equal to twice that of the shift produced by the previous column. The first column will produce a shift of Δ, the second column a shift of 2Δ, the third column a shift of 4Δ, and so on, then producing a binary system. We must devise a set of optics to replace Auxiliary Mirror II and perform this function, which we will tackle in Section III.

By shifting the spots, we can control at which row any given beam reaches the output turning mirror, and we associate each row with a different output. The number of possible outputs is determined by the total number of possible shifts for a given number of bounces. In the design of Fig. 2, a shift is made every time the light goes to the SDD, but this can only happen every four bounces. Thus, the number of outputs N is given by:

$$N_{\text{binary}} = 2^{m/4} = 2^{1/4}2^m \tag{1}$$

where m is the number of bounces. So, to implement a 1024 $\times$ 1024 system we would need a 40-bounce system ($2^{40/4} = 1024$).

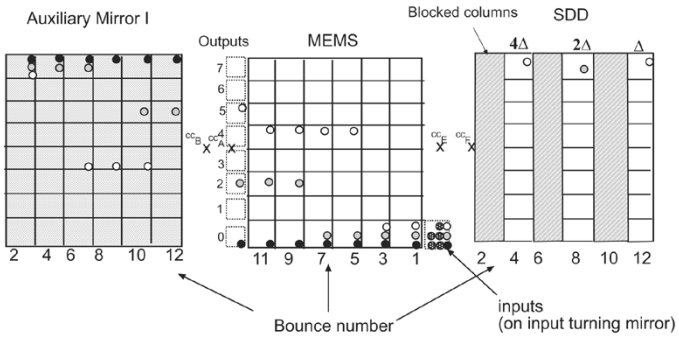

Fig. 3. Spot pattern for multiple inputs in the binary White cell-based optical switch.

We present a 12-bounce system in Fig. 3 to illustrate the operation. Here we can see eight different beams incident on the input turning mirror. The rest of the spot patterns for three of those beams are indicated. The MEMS, Auxiliary Mirror I, and the SDD are each divided into a grid of eight rows (for eight possible output locations) and six columns (for each possible bounce on the auxiliary mirror or SDD). Each region on this grid the MEMS mirror array is a group of eight micromirrors, so that each beam lands on a different micromirror on each bounce and can be directed either to the SDD or to Auxiliary Mirror I. The number of columns on the SDD is $(m/4)$, and will, thus, determine the number of possible outputs. An equal number of columns are then "blocked" or unused. Every fourth bounce allows for a different shift, of Δ, 2Δ, 4Δ, etc., so 12 bounces will produce $2^3 = 8$ different outputs for each input.

The figure shows the paths of three particular input beams (white, gray, and black) and eight possible outputs (numbered 0 to 7 on the figure). Initially, all three input beams start on row 0. Remember that, according to the connectivity diagram of Fig. 2, an input can only go to the EF White Cell every fourth bounce (those would be the fourth, eighth, and twelfth bounces). So, let us assume that we need to send the "white" beam to the fifth output. Therefore, we will need to send the "white" beam to the SDD on the fourth and twelfth bounces, which correspond to displacements of 4Δ and Δ, respectively. The "white" beam starts bouncing in the AB White Cell (i.e., the micromirrors on the MEMS array are tilted to the $-\theta$ position), until it is sent to the SDD on the fourth bounce (i.e., the micromirror is tilted to $+\theta$). Then, the "white" beam goes through the SDD, which for that particular column has a value of 4Δ, and will send the output back to the MEMS on the fourth row instead of the zeroth row. We then keep bouncing the "white" beam in the AB White cell, until the twelfth bounce, when we again send the input to the SDD. Now, the beam will land in the column with the shift value of Δ, where it goes through the SDD and is shifted by an additional distance Δ. In a similar way, we can send the "gray" beam to the second output and the "black" beam to the zeroth output.

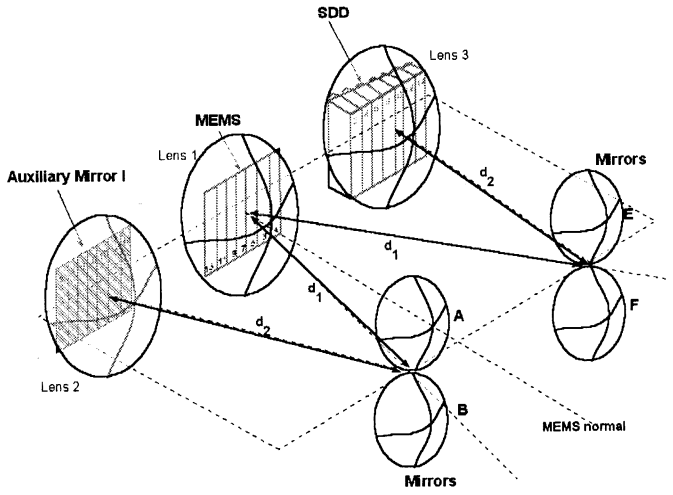

Fig. 4. SDD substitution for Auxiliary Mirror II in the binary White Cell.

III. SDD Design

In this section, we will describe how to design our SDD, which will be substituted for Auxiliary Mirror II. The SDD will displace each beam that goes into it such that its spot pattern is shifted by the appropriate amount on the MEMS plane.

To find an appropriate geometry, we will assume that the SDD may have any arbitrary shape. This shape, however, has to form a focused spot on a micromirror on the MEMS micromirror array. The SDD must also cause the light beam to be translated to a different row on the MEMS plane.

In Fig. 4, we show the binary White cell with Auxiliary Mirror II replaced by an arbitrary SDD. We removed the marks for the positions of the centers of curvature, as well as the angle separation marks between the different axes to simplify the figure. We can see that the distance between the MEMS mirror and the spherical mirrors AB (and EF) is d_1, and that the distance between the spherical mirrors and Auxiliary Mirror I (or the SDD) is defined as d_2. We will use this schematic to describe the design of the SDD.

In order to describe the row translation and the focusing of the beams on the MEMS plane, and on the different elements on the binary cell, we will use 3×3 ray matrices to include the effects of any element being tilted with respect to the optical axis [11].

The basic matrices used in this section are as follows:

$$T_1 = \begin{bmatrix} 1 & d_1 & 0 \\ 0 & 1 & 0 \\ 0 & 0 & 1 \end{bmatrix}$$

is the translation matrix between Lens 1 and spherical mirror A, B, E or F.

$$T_2 = \begin{bmatrix} 1 & d_2 & 0 \\ 0 & 1 & 0 \\ 0 & 0 & 1 \end{bmatrix}$$

is the translation matrix between Auxiliary Mirror I (or SDD) to Mirror A and B (or E and F).

$$M_A = \begin{bmatrix} 1 & 0 & 0 \\ -\dfrac{1}{f_a} & 1 & 0 \\ 0 & 0 & 1 \end{bmatrix}$$

is the matrix for spherical Mirror A, where f_a is its focal length, and similarly for M_B, M_C, and M_D:

$$L_1 = \begin{bmatrix} 1 & 0 & 0 \\ -\dfrac{1}{f_1} & 1 & 0 \\ 0 & 0 & 1 \end{bmatrix}$$

is the matrix for Lens 1, where f_1 is its focal length, and similarly for L_2 and L_3.

Furthermore, we will assign a generalized matrix to the SDD.

$$X = \begin{bmatrix} o & p & u \\ q & r & v \\ s & t & w \end{bmatrix}$$

is the general matrix for our SDD.

The value of elements o through w of Matrix X will define the optical element(s) needed to replace Auxiliary Mirror II and produce the desired shifts.

Next, we need to define the set of imaging conditions that must be satisfied for the double White cell. These conditions are stated as follows.

i) Mirror A images onto Mirror B via Auxiliary Mirror I.
ii) The MEMS mirror images onto Auxiliary Mirror I via Mirror A.
iii) Mirror E images onto Mirror F via the SDD.
iv) The MEMS mirror images onto the original plane of Auxiliary Mirror II via Mirror E. This plane will serve as a reference point, but is not necessarily at the entrance to the SDD as we will show.
v) Mirror A(B) images onto Mirror E(F) via the MEMS mirror.
vi) The MEMS mirror images onto itself via the SDD.

These conditions will be used to design the SDD as well, to determine the values of the focal lengths of the different lenses and spherical mirrors used and the distances d_1 and d_2. The plane of Auxiliary Mirror II refers to the original position at which this auxiliary mirror was found before being replaced by the SDD. This position will serve as a reference as to where to place the input/output plane of the SDD.

Our first condition to be analyzed is that Mirror A be imaged onto Mirror B. To establish this requirement, we calculate the system matrix C_1 from Mirror A to B, going through Auxiliary Mirror I which is given by multiplying together the matrices for each element in the path

$$C_1 = T_2 L_2 L_2 T_2. \tag{2}$$

The result is

$$C_1 = \begin{bmatrix} 1 - \dfrac{2d_2}{f_2} & \left(1 - \dfrac{2d_2}{f_2}\right) d_2 + d_2 & 0 \\ -\dfrac{2}{f_2} & 1 - \dfrac{2d_2}{f_2} & 0 \\ 0 & 0 & 1 \end{bmatrix}. \tag{3}$$

In order to have imaging from Mirror A to Mirror B of this particular path, the element $C_1[1, 2]$ has to be zero. Solving that equation for f_2 we obtain the solution

$$f_2 = d_2. \tag{4}$$

Now, we have to consider the requirement that an image on the MEMS mirror be imaged onto Auxiliary Mirror I via Mirror A (imaging condition ii). The system matrix for this case is

$$C_2 = L_1 T_1 M_A T_2 L_2. \tag{5}$$

Using the condition $f_2 = d_2$ in (5) we end up with the following matrix:

$$C_2 = \begin{bmatrix} -\dfrac{d_1}{d_2} & d_2 - \dfrac{d_2 d_1}{f_a} + d_1 & 0 \\ \dfrac{d_1}{d_2 f_1} - \dfrac{1}{d_2} & -\dfrac{d_2}{f_1} + \dfrac{d_2 d_1}{f_a f_1} - \dfrac{d_2}{f_a} - \dfrac{d_1}{f_1} + 1 & 0 \\ 0 & 0 & 1 \end{bmatrix}. \tag{6}$$

To obtain an imaging condition we need to set element $[1, 2]$ to zero

$$f_a = \frac{d_2 d_1}{d_2 + d_1}. \tag{7}$$

Because of the symmetry of the White cell, the focal length of Mirror A is the same as the focal length of Mirror B, similarly the focal length of lens 3 is equal to d_2.

Next, we calculate imaging condition iii: Mirror E images into Mirror F via the X element. The system matrix for this condition is

$$C_3 = T_2 L_3 X L_3 T_2 \tag{8}$$

which gives the following matrix:

$$C_3 = \begin{bmatrix} d_2 q - r & d_1^2 q & d_1 v \\ q - \dfrac{o}{d_2} + \dfrac{p}{d_2^3} - \dfrac{r}{d_2} & d_2 q - o & v - \dfrac{u}{d_2} \\ s - \dfrac{t}{d_2} & s d_2 & w \end{bmatrix}. \tag{9}$$

In order to have imaging, we again have to set element $C_3[1, 2]$ to zero. Because d_1 is a distance (that is not zero), element q of the X matrix has to be zero. Also, element $C_3[1, 3]$ represents a displacement in the image, (in this case the image of Mirror E on Mirror F). By setting v to zero, we produce no offset on the light imaging from Mirror E onto F, preventing walk-off.

The next imagining condition is to image the MEMS mirror onto the plane of the Auxiliary Mirror II. Condition iv helps us to find the focal lengths for spherical mirrors E and F. This system can be represented by the following equation:

$$C_4 = L_1 T_1 M_E T_2 L_3 \tag{10}$$

which produces the matrix

$$C_4 = \begin{bmatrix} -\dfrac{d_1}{d_2} & d_2 - \dfrac{d_2 d_1}{f_e} + d_1 & 0 \\ \dfrac{d_1}{d_2 f_1} - \dfrac{1}{d_2} & \dfrac{d_2 d_1}{f_e f_1} - \dfrac{d_2}{f_1} - \dfrac{d_2}{f_e} - \dfrac{d_1}{f_1} + 1 & 0 \\ 0 & 0 & 1 \end{bmatrix}. \tag{11}$$

Again, element $C_4[1, 2]$ has to be set to zero. Solving for f_e, we have

$$f_e = \frac{d_2 d_1}{d_2 + d_1}. \tag{12}$$

Because of the symmetry between spherical Mirrors E and F, the focal length of spherical Mirror F is set equal to the focal length of spherical Mirror E.

Next, we will image Mirror B onto E going through the MEMS mirror. For this condition, the matrix system is defined as

$$C_5 = T_1 L_1 L_1 T_1 \tag{13}$$

which gives us the following matrix:

$$C_5 = \begin{bmatrix} -\dfrac{2d_1}{f_1} + 1 & \left(\dfrac{2d_1}{f_1} + 1\right) d_1 + d_1 & 0 \\ -\dfrac{2}{f_1} & -\dfrac{2d_1}{f_1} + 1 & 0 \\ 0 & 0 & 1 \end{bmatrix}. \tag{14}$$

Setting element $C_5[1, 2]$ equal to zero gives us $f_1 = d_1$.

Now, we analyze our final imaging condition, which is that the MEMS has to image onto itself going through the SDD. The system matrix is

$$C_6 = L_1 T_1 M_E T_2 L_3 X L_3 T_2 M_F T_1 L_1 \tag{15}$$

which gives us

$$C_6 = \begin{bmatrix} o & p\dfrac{d_1^2}{d_2^2} & -u\dfrac{d_1}{d_2} \\ 0 & r & 0 \\ -s & -t & w \end{bmatrix}. \tag{16}$$

In order to keep the symmetry between the different arms on the White cell, we will set $d_2 = d_1$. We also set variable p to zero to obtain imaging.

Element o is the magnification of one spot on the MEMS to the next, which would typically be set to 1. Because the third element of the output vector is 1, and element w is also 1, elements s and t should also be set to zero. The element u gives the shift of the spots on the MEMS plane. So, by controlling the value of u, we will be able to control the displacement caused by the SDD.

The final matrix that we desire for our SDD is as follows:

$$\text{SDD} = \begin{bmatrix} 1 & 0 & -u \\ 0 & 1 & 0 \\ 0 & 0 & 1 \end{bmatrix}. \tag{17}$$

Our goal is to achieve shifts in the spot images on the MEMS, and that position offset depends on the u element of SDD. This offset will give us the row shift that we explained in the second section of this paper.

In the following section, we examine various physical implementations that produce the desired matrix for SDD.

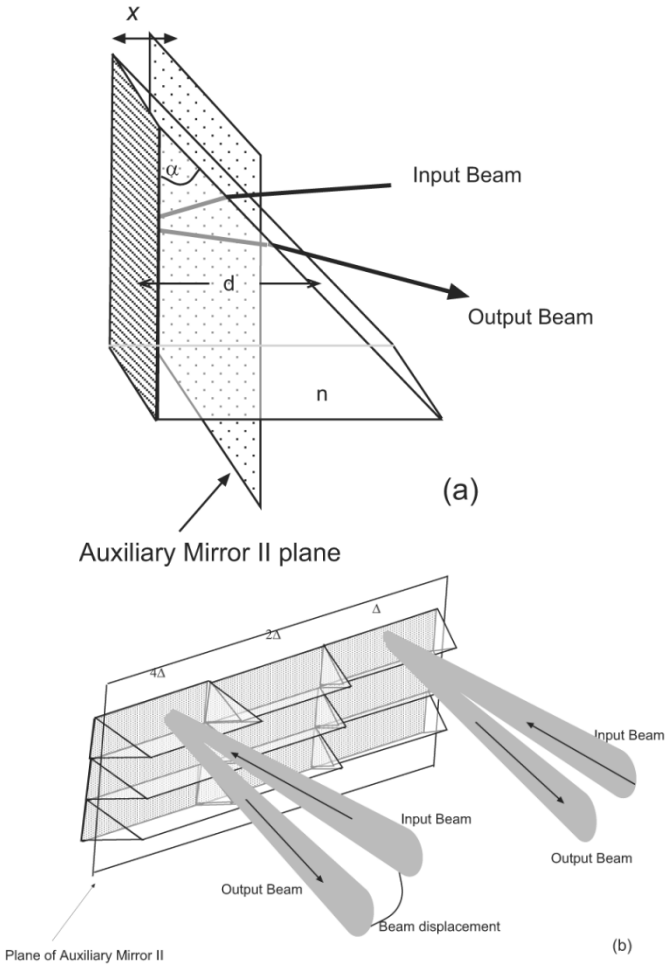

Fig. 5. Substitution of X element by a prism; (a) single element; (b) array.

IV. Physical Implementations of the SDD

Now, we analyze different shapes trying to fulfill the conditions previously mentioned. The key goals are that the imaging conditions are all maintained, and that the element u on the X matrix produces the proper shift in the spots on the MEMS.

A. Prism

Our first geometry is that of a prism shown in Fig. 5(a). This prism would be element X, and would replace one column of Auxiliary Mirror II. Here, we have a right-angle prism of apex angle α and refractive index n. It extends both in front of and in back of the original plane of Auxiliary Mirror II, as we will see shortly. The distance d is the thickness of the prism, which varies with height, and x is the distance between the original plane of Auxiliary Mirror II and the back plane of the prism.

Let us assume a nonsmall angle approximation. The ray matrix for the light coming in and out of the prism will be

$$P = \begin{bmatrix} o & p & u \\ q & r & v \\ s & t & w \end{bmatrix} = \begin{bmatrix} 1 & \dfrac{2d}{n} & 2d\left(\dfrac{1}{n}-1\right)\tan\alpha \\ 0 & 1 & 0 \\ 0 & 0 & 1 \end{bmatrix}. \quad (18)$$

This element P is substituted for X in (15). As we can see, we have achieved the zero value in the v element. We also notice that the u element (element $[1, 3]$, which produces the spot displacement) is a function of the prism thickness, the apex angle, and the refractive index of the material.

Also, we can see that the element $P[1, 2]$ cannot be zero. This means that, to obtain an imaging condition, the position of the prism has to be different from that of Auxiliary Mirror II. This new position is defined by the following:

$$P_{\text{new\_position}} = \begin{bmatrix} 1 & x & 0 \\ 0 & 1 & 0 \\ 0 & 0 & 1 \end{bmatrix} \times \begin{bmatrix} 1 & \dfrac{2d}{n} & 2d\left(\dfrac{1}{n}-1\right)\tan\alpha \\ 0 & 1 & 0 \\ 0 & 0 & 1 \end{bmatrix}. \quad (19)$$

The first matrix is a displacement matrix, where x is the distance from the Auxiliary Mirror II to the back plane of the prism as seen in Fig. 5(a). The second matrix is that of the prism. Equation (19) simplifies to:

$$P_{\text{new\_position}} = \begin{bmatrix} 1 & \dfrac{2d}{n}+x & 2d\left(\dfrac{1}{n}-1\right)\tan\alpha \\ 0 & 1 & 0 \\ 0 & 0 & 1 \end{bmatrix}. \quad (20)$$

From (20), we now can calculate a distance x that will produce imaging for our prism configuration. This distance is $x = -2d/n$ from the Auxiliary Mirror II plane.

Unfortunately, the prism has a big disadvantage inherent in its shape. The thickness of the prism changes depending on the place where the light strikes the prism. If the light goes in near the base, it will have a bigger displacement than light that strikes the prism higher up. In order to decrease this dependence on the prism height, one possibility to implement the SDD as a series of small prisms is shown in Fig. 5(b).

B. Parallelogram Prism

A better solution is to eliminate the thickness variable d in (20) that we had in the previous design. We propose a parallelogram prism element as shown in Fig. 6.

We can see that we now have two tilted surfaces, and the thickness of the double-prism is the same for every spot. For light coming in and out of the parallelogram the ray matrix is

$$P_2 = \begin{bmatrix} 1 & \dfrac{2d}{n} & 2d\left(\dfrac{1}{n}-1\right)\tan\alpha \\ 0 & 1 & n\tan\alpha \\ 0 & 0 & 1 \end{bmatrix}. \quad (21)$$

As stated before, element $[1, 3]$ represents the shift in position, and element $[2, 3]$ represents an angular offset that should be zero. It will be noted that, in this case, it is not, in fact, zero. This angular offset affects the imaging of Mirror E onto Mirror F, so as long as these two mirrors are big enough and no light is lost in any bounce this offset can be tolerated. Nevertheless, a better solution with no angular offset is needed.

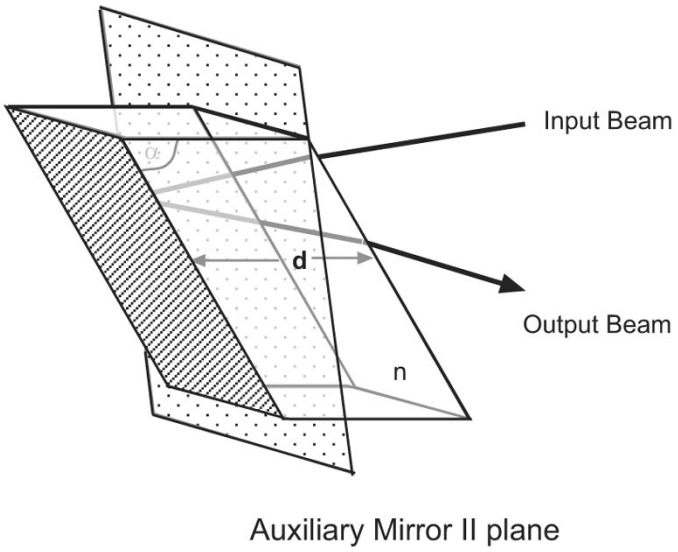

Fig. 6. Parallelogram prism.

C. Mirror and Lenses

Another approach to creating the spot displacements is described in this section. Let us consider a combination of a lens and a tilted spherical mirror as shown in Fig. 7(a). Here, d_{SDD} is the distance between the lens and the tilted spherical mirror, θ is the tilt angle of the spherical mirror, f_{SDD} is the focal length of the mirror, and f_l is the focal length of the lens.

Now, let us assume that the lens is in the plane of Auxiliary Mirror II. The light travels through lens f_l, translates a distance d_{SDD}, is reflected by a tilted spherical mirror of focal length f_{SDD}, and goes back the same way. The resulting matrix is:

$$\mathrm{SDD} = \begin{bmatrix} 1 & 0 & 0 \\ -\dfrac{1}{f_l} & 1 & 0 \\ 0 & 0 & 1 \end{bmatrix} \begin{bmatrix} 1 & d_{\mathrm{sdd}} & 0 \\ 0 & 1 & 0 \\ 0 & 0 & 1 \end{bmatrix} \begin{bmatrix} 1 & 0 & 0 \\ -\dfrac{1}{f_{\mathrm{sdd}}} & 1 & 2\theta \\ 0 & 0 & 1 \end{bmatrix} \times \begin{bmatrix} 1 & d_{\mathrm{sdd}} & 0 \\ 0 & 1 & 0 \\ 0 & 0 & 1 \end{bmatrix} \begin{bmatrix} 1 & 0 & 0 \\ -\dfrac{1}{f_l} & 1 & 0 \\ 0 & 0 & 1 \end{bmatrix}. \quad (22)$$

If we take $f_l = d_{\mathrm{SDD}}$ the result simplifies as follows:

$$\mathrm{SDD} = \begin{bmatrix} -1 & \left(1 - \dfrac{d_{\mathrm{sdd}}}{f_{\mathrm{sdd}}}\right) d_{\mathrm{sdd}} + d_{\mathrm{sdd}} & 2d_{\mathrm{sdd}}\theta \\ 0 & -1 & 0 \\ 0 & 0 & 1 \end{bmatrix}. \quad (23)$$

For imaging, element $\mathrm{SDD}[1, 2]$ must be zero, making $f_{\mathrm{SDD}} = d_{\mathrm{SDD}}/2$. Thus, (23) simplifies to

$$\mathrm{SDD} = \begin{bmatrix} -1 & 0 & 2d_{\mathrm{sdd}}\theta \\ 0 & -1 & 0 \\ 0 & 0 & 1 \end{bmatrix}. \quad (24)$$

As we can see, (24) is very similar to our goal matrix, shown in (17). The only difference is a factor -1, which implies an inverted image that does not affect the performance of our system. Now, the displacement in the beam position on the MEMS plane is given by element $[1, 3]$, that is $-2d_{\mathrm{SDD}}\theta$, from (24).

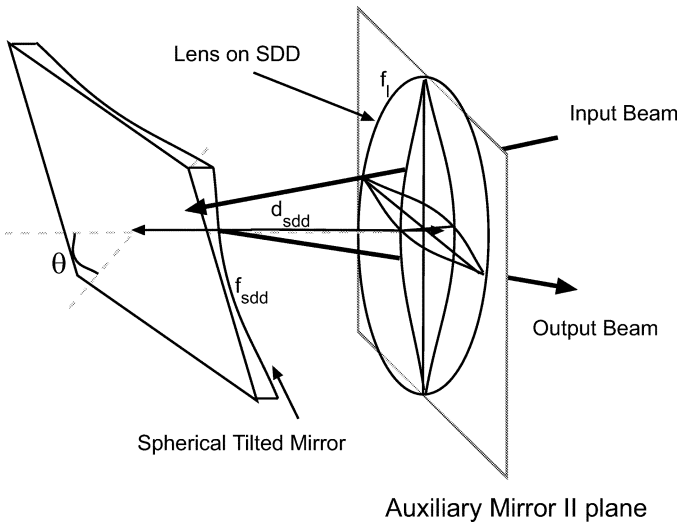

(a)

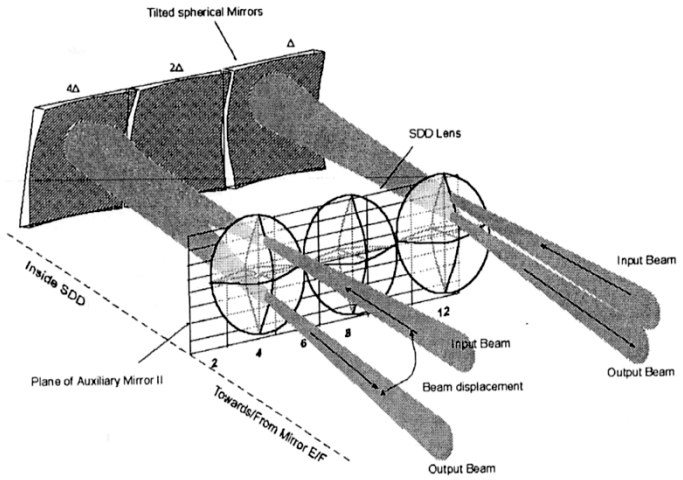

(b)

Fig. 7. (a) Lens and spherical mirror combination; (b) An SDD consisting of a lens and an array of tilted spherical mirrors.

As was mentioned earlier, each column on Auxiliary Mirror II will be replaced by a different SDD. Each SDD produces a different shift, so each has its spherical mirror tilted by a different angle θ, or is located at a different distance d_{SDD} from the lens, or a combination of both. To keep the transit times equal, however, it is desirable to fix d_{SDD} and vary θ.

Fig. 7(b) shows one possible implementation of the proposed SDD. The lenses are in the plane of Auxiliary Mirror II. The spots form in columns on this plane. Spots in the column labeled "12" should be shifted by one pixel in the SDD, spots in the column labeled "8" (for eighth bounce) should be shifted by two pixels, spots in the column labeled "4" should be shifted by four pixels, and so on. The overall mirror shapes may be strips with a spherical surface as shown, or a series of microspherical mirrors.

D. Pitch Calculation

So far, we have found three designs that can produce a shift of the beam position on the MEMS plane by changing the angle of reflection on the SDD. We will focus on the last design because it is the SDD system that looks most promising to implement.

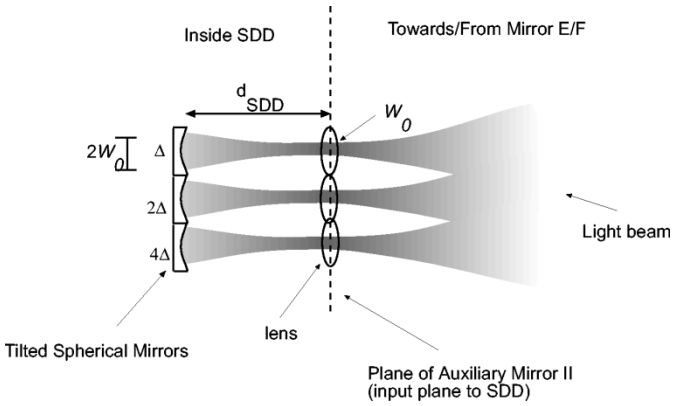

Fig. 8. Top view. Light diverges inside the SDD.

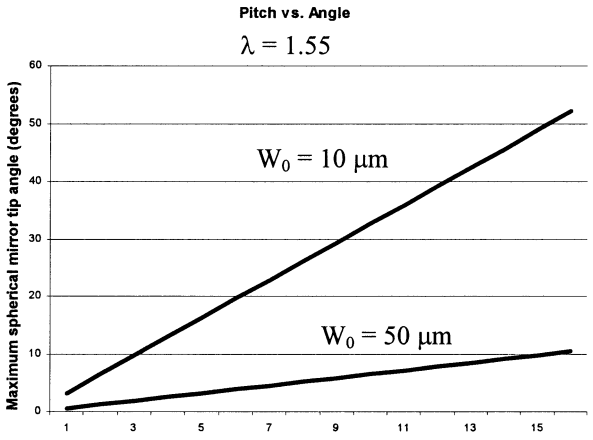

Fig. 9. Value of θ for different pitches using the tilted mirror design of Fig. 7.

In this section, we will define in more detail some of the physical characteristics needed to cause a predetermined shift of the beams at the MEMS plane.

Let us analyze the tilted mirror configuration of Fig. 7(a) first. As stated before, we will fix the distance $d_{\rm SDD}$, and change θ for different columns. There is, however, a limit on the size of θ. To avoid excessive aberration, we would like to keep θ less than 10°.

To calculate how big the angle of reflection on the SDD should be, we need to relate the displacement caused by the SDD to the micromirror size on the MEMS micromirror array. We will define the pitch between micromirrors as Δ, so for the simplest case, in which the SDD has to cause a displacement of one row, the relation between the mirror pitch and the SDD is stated as follows:

$$\Delta = 2d_{\rm SDD}\theta. \tag{25}$$

Independent of the size of Δ, for 99.99% of the beam's power to be contained inside the dimensions of the micromirror (and, thus, minimize the loss during each bounce), the micromirror has to be at least four times the size of beam spot (assuming Gaussian beams). So Δ can also be expressed as:

$$\Delta = 4W_0 \tag{26}$$

where W_0 is the spot size of the beam at the MEMS plane, (we will use W_0 instead of the usual variable w_0, so the spot size is not confused with element w of the matrix X of Section III).

To calculate the distance $d_{\rm SDD}$, we will refer to Fig. 8. It is a top view of the SDD. As we can see when light enters the SDD, it has a size W_0 at the plane of Auxiliary Mirror II. The light will then diverge as it travels toward the spherical tilted mirror. This divergence is described by the formula [1]

$$W^2(d_{\rm SDD}) = W_0^2\left(1 + \frac{d_{\rm SDD}^2}{z_0}\right) \tag{27}$$

where $W(d_{\rm SDD})$ is the final beam radius, W_0 is the beam waist, which occurs at the input plane, $d_{\rm SDD}$ is the distance from the beam waist to the tilted spherical mirror, and z_0 is the Rayleigh distance $\pi W_0^2/\lambda$, where λ is the wavelength.

The final size to which the light beam can diverge inside the SDD is defined by the geometry of the SDD itself. The spot size at the spherical mirrors cannot be larger than $2W_0$, otherwise the beam in one column will overlap to an adjacent column. (The spherical mirrors are twice the size of the pitch of the input columns on the plane of Auxiliary Mirror II, and they do not overlap because alternate columns on the SDD are not used, Fig. 3).

So, from (27), and assuming the condition that $W^2(d_{\rm SDD}) = 2W_0$, we solve for $d_{\rm SDD}$

$$d_{\rm SDD} = \sqrt{3}\,\frac{\pi W_0^2}{\lambda}. \tag{28}$$

Substituting (28) into (26) and solving for θ in degrees yields

$$\theta = \frac{4\lambda}{2\sqrt{3}\pi W_0}\left(\frac{180}{\pi}\right). \tag{29}$$

Equation (29) describes the value of the mirror tilt angle θ in degrees for a displacement Δ.

Fig. 9 graphs the angle (in degrees) needed to cause a particular displacement from Δ to 10Δ at a wavelength of 1.55 μm for different beam waists using the tilted mirror design. We can see that for $W_0 = 10$ μm, θ exceeds 10° for displacements larger than 4Δ. This situation improves when W_0 is increased up to 50 μm. For displacements larger than 128Δ, the beam waist at the input plane of the SDD has to be $\sim$1 mm.

V. Summary and Conclusion

We have presented a new architecture to perform optical switching with a modified White Cell. We have shown that our implementation can be used as an optical interconnection device that is binary; the number of outputs to which a given input can be shifted is given by $2^{m/4}$, where m is the number of bounces a beam makes in a dual White cell. We assumed a micro-electromechanical systems (MEMS) micromirror array in which the micromirrors can be tilted to two different positions, for the purposes of discussion. Some of the bounces can be directed either to an SDD or to a plane mirror. Each visit to the SDD translates the spot pattern of a particular input beam to a specific row. After the required number of bounces, each input is shifted to the appropriate output region.

Within each output region, beams may arrive at different points and from different angles. This was solved in two different ways: one combined all the beams to a single point and angle using a series of cascaded prisms and a total-internal-reflection waveguide, and the other used substrate-mode holograms as fanin devices.

We found three solutions for our SDD. The first one is a prism of apex α, and has a final displacement on the original MEMS spot position of $-2d(1/n-1)\tan(\alpha)$. The second is a parallelogram that also has a final displacement of $-2d(1/n-1)\tan(\alpha)$. Our third solution is an SDD formed by the combination of a lens and a spherical tilted mirror that give us a final displacement on the original position of MEMS spot of $-2d_{\mathrm{SDD}}\theta$.

The White cell approach is different from other 3-D photonic switches, in that the beams are directed to their appropriate outputs by fixed, stationary optics, not by the MEMS micromirrors. The MEMS device serves only to select the optics visited. Further, the White cell approach requires only a digital MEMS device, as opposed to an analog one. That is, the micromirrors need only tip to a small number of fixed positions (in this paper we assumed two), and furthermore the micromirror tilt angle does not have to be precisely controlled. If the micromirror tilt angle is off by a degree or two, that affects where on the spherical mirrors the light lands, but we emphasize it has no effect on the placement of subsequent spots. Thus, feedback and precise control of the micromirror tilt angle is not needed, and this feedback comprises the bulk of the complexity and the cost of existing 3-D switches.

One disadvantage of the White cell approach to optical switching is that it requires more pixels than the conventional 3-D switches. There is every reason to suppose, however, that very large MEMS micromirror arrays will become available in time, just as very large scale integrated circuits have become commonplace. Thus, we do not believe the MEMS device availability to be a show-stopper.

We also note that in the White cell, the MEMS mirror losses must be kept very small, because, unlike in other photonic switches, each beam strikes the MEMS multiple times. This means that MEMS for a White-cell based interconnection will require high-quality gold coatings, or possibly even dielectric high-reflectivity coatings. Although such devices are not currently commercially available, however, there should be no technological restriction in the future.

The White cell approach has the advantage of being very simple from a hardware point of view. The binary cell, for example, requires a MEMS, four spherical mirrors, three lenses, and an SDD, whether it is a 32×32 photonic switch or a 1024×1024 photonic switch. Only the SDD and the number of pixels on the MEMS change. Thus, the amount of hardware for a truly large photonic switch is not excessive.

Finally, although we have presented a binary system based on a two-state MEMS, it will be appreciated that with MEMS having more stable states, the number of inputs and outputs can be increased while the number of bounces is decreased. These higher-order systems will be discussed in a following work.

REFERENCES

[1] B. E. A. Saleh and M. C. Teich, *Fundamentals of Photonics*. New York: Wiley, 1991.

[2] D. K. Probst, L. G. Perrymore, B. C. Johnson, R. J. Blackwell, J. A. Priest, and C. L. Balestra, "Demonstration of an integrated, active 4×4 photonic crossbar," *IEEE Photon. Technol. Lett.*, vol. 4, pp. 1139–1140, Oct. 1992.

[3] M. Okuno, K. Kato, R. Nagase, A. Himeno, Y. Ohmore, and M. Kawachi, "Silica-based optical matrix switch integrating new switching units with large fabrication tolerance," *J. Lightwave Technol.*, vol. 17, pp. 771–780, May 1999.

[4] L. Y. Lin, E. L. Goldstein, and R. W. Tkach, "Free-space micromachines optical switches with submillisecond switching time for large-scale optical cross-connects," *IEEE Photon. Technol. Lett.*, vol. 10, pp. 525–527, Apr. 1998.

[5] J. E. Fouquet, "Waveguide-based optical cross-connect switches," in *OFC 2002 Tutorial*. Anaheim, CA: Optic. Soc. Amer., 2002.

[6] D. J. Bishop, C. R. Giles, and G. P. Austin, "The Lucent LambdaRouter: MEMS technology of the future here today," *IEEE Commun. Mag.*, vol. 40, pp. 75–79, Mar. 2002.

[7] J. White, "Long optical paths of large aperture," *J. Optic. Soc. Am.*, vol. 32, no. 5, pp. 285–288, 1942.

[8] B. L. Anderson and C. D. Liddle, "Optical true-time delay for phased array antennas: Demonstration of a quadratic White cell," *Appl. Opt.*, vol. 41, pp. 4912–4921, 2002.

[9] B. L. Anderson, V. Argueta-Diaz, F. Abou-Galala, G. Radhakrishnan, and R. Higgins, "Optical cross-connect switch based on tip/tilt micromirrors in a White cell," *IEEE J. Select. Topics Quantum Electron.*, vol. 9, Mar.-Apr. 2003.

[10] J. Stuart, A. Collins, and B. L. Anderson, "Device and method for producing optically-controlled incremental time delays," U.S. Patent No. 6388615, 2002.

[11] W. Brouwer, *Matrix Methods in Optical Instrument Design*. New York: Benjamin Press, 1964.

Victor Argueta-Diaz received the B.S. degree in telecommunication engineering from the National Autonomous University of Mexico, Mexico City, Mexico, in 1999 and the M.S. degree in electrical engineering from The Ohio State University, Columbus, in 2002.

He spent two years in the industry, working on optochemical sensors and wireless communication. He is currently in the Department of Electrical Engineering, The Ohio State University. His current research interests include devices for optical communication systems, photonic crystals, and optical sensors.

Betty Lise Anderson (S'75–M'79–SM'95) received the B.S. degree in electrical engineering from Syracuse University, Syracuse, NY, in 1978 and the M.S. and Ph.D. degrees in material science and electrical engineering from the University of Vermont, Burlington, in 1988 and 1990, respectively.

She spent nine years in the industry, including at Tektronix, Inc., Beaverton, OR, GTE Laboratories, Waltham, MA, and Draper Laboratories, Cambridge, MA. She is currently with the Department of Electrical Engineering, The Ohio State University, Columbus. Her current research interests include analog optical signal processing, devices for optical communication systems, coherence, and semiconductor devices.

Prof. Anderson is a member of the Optical Society of America and the Society for Photoinstrumentation Engineers.